Gamma rays and neutrinos from the Crab Nebula produced by pulsar accelerated nuclei

W. Bednarek* and R.J. Protheroe

Department of Physics and Mathematical Physics, University of Adelaide, Adelaide, SA 5005, Australia
Permanent address: University of Łódź, 90-236 Łódź, ul. Pomorska 149/153, Poland.

We investigate the consequences of the acceleration of heavy nuclei (e.g. iron nuclei) by the Crab pulsar. Accelerated nuclei can photodisintegrate in collisions with soft photons produced in the pulsar's outer gap, injecting energetic neutrons which decay either inside or outside the Crab Nebula. The protons from neutron decay inside the nebula are trapped by the Crab Nebula magnetic field, and accumulate inside the nebula producing gamma-rays and neutrinos in collisions with the matter in the nebula. Neutrons decaying outside the Crab Nebula contribute to the Galactic cosmic rays. We compute the expected fluxes of gamma-rays and neutrinos, and find that our model could account for the observed emission at high energies and may be tested by searching for high energy neutrinos with future neutrino telescopes currently in the design stage.

PACS numbers: 98.70.Rz, 98.58.Mj, 95.85.Ry, 97.60.Gb, 98.70.Sa.

The Crab Nebula is a well established γ-ray source with a complex spectrum extending up to at least TeV energies [1]. Its emission below a few tens of MeV is interpreted as synchrotron emission by electrons with energies up to $\sim 10^{15-16}$ eV in the Crab Nebula magnetic field of strength $\sim 3 \times 10^{-4}$ G [2]. These models interpret the emission at higher energies as being due this same population of electrons by inverse Compton scattering (ICS) of synchrotron photons (SSC models). The TeV γ-ray emission might also originate near (but above) the Crab pulsar light cylinder as a result of ICS scattering of infrared photons produced in one of the pulsar's outer gaps by $e^{\pm}$ pairs escaping from another outer gap [3]. The possible importance of hadronic processes as sources of γ-rays inside the Crab Nebula has also been considered by Cheng et al. [4] who calculated the high energy γ-ray fluxes assuming that relativistic protons accelerated in the Crab pulsar outer gap interact with the matter inside the Nebula, and note that this process may contribute in the TeV γ-ray range.

In this Letter, we analyze the consequences of acceleration of heavy nuclei in the pulsar magnetosphere as a possible mechanism of energetic radiation from the Crab Nebula. The importance of photodisintegration of nuclei is determined by the reciprocal mean free path which we calculate using cross sections of Karakuła & Tkaczyk [5] and show in Fig. 1 for nuclei with atomic mass numbers between 4 and 56 during propagation in the radiation field supposed to be present in the outer gap of the Crab pulsar. Ho [6] has shown that the total luminosity and spectrum of the outer gap radiation is not strongly dependent on P. For $P = 33$ ms we adopt the photon number density given by Eq. 7.1 in Paper II of Cheng et al. [7], and for other periods we scale this by $r_{\rm LC}^{-3}$. We assume this radiation is produced by cascading due to electrons and positrons accelerated in the gap, and so is

highly anisotropic and directed across the gap (in both directions). The dimension of the outer gap is of the order of the radius of the light cylinder, $l_{\mathrm{gap}} \approx r_{\mathrm{LC}} = c/\Omega$. For the case of the Crab pulsar, $r_{\mathrm{LC}} \approx 1.5 \times 10^8$ cm, and it is evident from Fig. 1 that multiple photodisintegrations of primary Fe nuclei will occur provided they can be accelerated to Lorentz factors above $\sim 10^3$. To check whether pion photoproduction and $e^\pm$ pair production by Fe nuclei are important energy loss mechanisms in the outer gap, we compute also the mean interaction length for pion photoproduction using the cross section given by Stecker [8], and the energy loss length for pair production using the approximations given by Chodorowski et al. [9]. The results are shown in Fig. 1. It is clear that these processes are not important loss mechanisms compared to photodisintegration, e.g the pair production energy loss length is two orders of magnitude longer than the length of the gap.

We assume that Fe nuclei can escape from the polar cap surface of the Crab pulsar, and move along magnetic field lines to enter the outer gap where they can be accelerated in the outer gap potential as in the model of Cheng et al. [7] and Ho [6]. The nuclei accelerated in the outer gap will interact with photons either producing secondary $e^\pm$ pairs (with negligible loss of energy) or extracting a nucleon. The pairs could eventually saturate the electric field of the gap although this is far from certain. We shall assume that for some reason the field is not shorted. Possibilities include: (a) nuclei, having much larger Larmor radii and much lower synchrotron and curvature losses than electrons, more easily drift across the magnetic field lines away from the region of the gap where they had produced pairs; (b) the secondary $e^\pm$ pairs may not be able to saturate the electric field in the outer gap which is close to the light cylinder since the Goldreich & Julian [10] density tends to infinity where the gap approaches the light cylinder.

In order to obtain the energy spectrum of neutrons extracted from Fe nuclei, $N_n(\gamma_n)$, we simulate their acceleration and propagation through the outer gap using a Monte Carlo method. To obtain the rate of injection of neutrons per unit energy we multiply $N_n(\gamma_n)$ by the number of Fe nuclei injected per unit time, $\dot{N}_{\mathrm{Fe}}$, which can be simply related to the total power output of the pulsar $L_{\mathrm{Crab}}(B, P)$ [11],

$$\dot{N}_{\mathrm{Fe}} = \xi L_{\mathrm{Crab}}(B, P)/Z\Phi(B, P), \qquad (1)$$

where ξ is the parameter describing the fraction of the total power taken by relativistic nuclei accelerated in the outer gap, $Z = 26$ is the atomic number of Fe, B is the surface magnetic field, P is the pulsar's period, and

$$\Phi(B, P) \approx 5 \times 10^{16} \left(\frac{B}{4 \times 10^{12}\,\mathrm{G}} \right) \left(\frac{P}{1\,\mathrm{s}} \right)^{4/3} \mathrm{V} \qquad (2)$$

is the potential difference across the outer gap [4]. We assume $B = 4 \times 10^{12}$ G.

Soon after the supernova explosion, when the nebula was relatively small, nearly all energetic neutrons would be expected to decay outside the nebula. However, at early times we must take account of collisions with matter. The optical depth may be estimated from $\tau_{nH} \approx \sigma_{pp} n_H r \approx 8.6 \times 10^{14} M_1 v_8^{-2} t^{-2}$, where $M = M_1 M_\odot$ is the mass ejected during the Crab supernova explosion in units of solar masses, $r = vt$, $n_H = M/(4/3\pi r^3 m_p)$ is the number density of target nuclei, and $v = 10^8 v_8$ cm s^{-1} is the expansion velocity of the nebula. We note that $\tau_{nH} = 1$ at $t \approx 0.93 M_1^{1/2} v_8^{-1}$ y.

The number and spectrum of relativistic protons from neutron decay at the present time is determinated by the injection rate of neutrons into the Crab Nebula integrated over time since the pulsar's birth. We estimate the evolution of the Crab pulsar's period from birth to the present time taking account of magnetic dipole radiation energy losses and gravitational energy losses for an ellipticity of 3×10^{-4} [12]. Magnetic dipole losses determine the pulsar period at present, but the initial period is determined largely by gravitational losses and is probably shorter than ~ 10 ms. Hence, we consider two initial periods: 5 ms, and 10 ms.

The spectrum of protons from neutron decay outside the Crab Nebula is given by

$$N_p^{\text{out}}(\gamma_p, t_{\text{CN}}) =$$
$$\int_0^{t_{\text{CN}}} dt \dot{N}_{\text{Fe}}(t) N_n(\gamma_p, t) e^{-\tau_{nH}(t)} e^{-vt_{\text{CN}}/c\gamma_p \tau_n} \qquad (3)$$

where $\tau_n \approx 900$ seconds is the neutron decay time, and we make the approximation that the Lorentz factor of protons is equal to that of parent neutrons, $\gamma_p \approx \gamma_n$.

The equation for the spectrum of protons injected inside the Crab Nebula is more complicated because we must take account of proton-proton collisions and adiabatic energy losses due to the expansion of the nebula. The Lorentz factor of these protons at time t after the explosion such that their present Lorentz factor is γ_p is given by

$$\gamma_p(t) \approx \gamma_p \frac{(t + t_{\text{CN}})}{2t K^{\tau_{pp}(t)}} \qquad (4)$$

where $\tau_{pp}(t)$ is the optical depth for collision of protons with matter between t and t_{CN}, and is given by $\tau_{pp}(t) \approx 1.3 \times 10^{17} M_1 v_8^{-3}(t^{-2} - t_{\text{CN}}^{-2})$, and $K \approx 0.5$ is the inelasticity coefficient in proton–proton collisions.

Since we are interested in protons interacting inside the nebula at the present time, we must also include those neutrons which decayed at locations outside the nebula at time t but which will be inside the nebula at time t_{CN}. Taking account of all these effects, we arrive at the formula below for the proton spectrum inside the nebula at time t_{CN},

$$N_p^{\text{in}}(\gamma_p, t_{\text{CN}}) = \gamma_p^{-1} \int_0^{t_{\text{CN}}} dt \dot{N}_{\text{Fe}}(t) e^{-\tau_{nH}(t)}$$

3

$$\times \left[N_n(\gamma_p(t), t)\gamma_p(t)[1 - \exp(-vt/c\gamma_p(t)\tau_n)] \right.$$

$$\left. + \int_t^{t_{\rm CN}} dt' N_n(\gamma_p(t'), t)\gamma_p(t') \frac{v \exp(-vt'/c\gamma_p(t')\tau_n)}{c\gamma_p(t')\tau_n} \right]. \quad (5)$$

The first term gives the contribution from neutrons decaying initially inside the nebula while second term gives the contribution from neutrons decaying at points initially outside the nebula which will be inside the nebula at time $t_{\rm CN}$.

We compute separately the spectra of protons from neutrons decaying inside and outside the Crab Nebula. In Fig. 2 proton spectra are shown for two initial periods and present nebula radii of 1 pc and 2 pc. To check if protons decaying inside will remain near where they were produced, or diffuse into the Galactic environment, we estimate their typical diffusion distance during time $t_{\rm CN}$, $x_{\rm dif} \approx (cr_L t_{\rm CN}/3)^{1/2}$, where $r_L = m_p\gamma_p c^2/eB$ is the Larmor radius, and we have used the minimum diffusion coefficient. For protons at the peak of the energy spectrum with $\gamma_p = 10^5$ in a magnetic field of the order of $B = 5 \times 10^{-6}$ G, the typical diffusion distance is $x_{\rm dif} \approx 1$ pc, which is comparable to the radius of the Crab Nebula. Hence protons which decayed inside, were probably trapped and accumulated inside the nebula. Protons from neutrons decaying outside the nebula will typically have higher energies and diffuse farther, thus escaping to become Galactic cosmic rays.

The protons which have accumulated inside the Crab Nebula since the pulsar was formed can produce observable fluxes of γ-rays and neutrinos. We compute the expected γ-ray spectra for four different models, taking various initial pulsar periods, present sizes and masses of the Crab Nebula. The fluxes may possibly be enhanced if protons are efficiently trapped by the dense filaments as suggested by Atoyan and Aharonian [13]. Filaments with density ~ 500 cm^{-3} are present in the Crab Nebula [14]. Therefore we introduce an effective density experienced by the protons inside nebula, $n_H^{\rm eff} = \mu n_H$, where n_H is defined above, and the parameter μ takes into account the possible effects of proton trapping by the filaments. The γ-ray spectra are computed in terms of a scaling model [15], and the photon fluxes expected at the Earth are shown in Fig. 3 for $\xi\mu = 1$, and are compared with observations of the Crab Nebula above 0.2 TeV. Results are shown for models I to IV having P_0, $r_{\rm CN}$ and M_1 as specified in Table I, and for a distance to the Crab Nebula of 1830 pc [14]. Comparison with the Whipple observations at 10 TeV allows us to place constraints on the free parameters of the model, and upper limits on $\xi\mu$ which are given in Table I as $(\xi\mu)_\gamma$. Note that it is usually argued for the standard pulsar model that the rate of injection of Fe nuclei into the pulsar magnetosphere should not cause the charge density to exceed the Goldreich & Julian density [10]. In the case of no additional currents flowing through the magnetosphere, this condition constrains the value of ξ to $\xi \approx 0.1$ for the Crab pulsar with period 33 ms. However, in the presence of

additional currents the value of ξ can be higher.

The question of the importance of hadronic interactions in the Crab Nebula can be settled by the detection of a neutrino signal from the Crab. In Fig. 4 we show the neutrino spectrum produced in collisions of protons with matter inside the Crab nebula for the models considered above, and compare this with the atmospheric neutrino background flux within $1°$ of the source direction [20]. It is clear that neutrino detectors with good angular resolution should be able to detect neutrinos at 10 TeV from the Crab Nebula if $\xi\mu$ is greater than $(\xi\mu)_\nu$ given in Table I. Note that in all cases $(\xi\mu)_\nu < (\xi\mu)_\gamma$ and so the possibility of ν detection is allowed by the existing γ-ray observations.

In the present paper we have not considered those nuclei which had survived propagation through the outer gap radiation field and were injected into the inner nebula region following magnetic field lines. These nuclei (and protons) are expected to accumulate in the inner part of the Crab Nebula were the magnetic fields are $\sim 2 \times 10^{-3}$ G measured in the synchrotron wisps which are located at ~ 0.2 pc [21]. The diffusion distance scale during the age of the Crab Nebula is ~ 0.3 pc for a Lorentz factor $\gamma_A = 10^6$ and $B = 10^{-3}$ G. This means that most nuclei will probably be confined to the inner part of the Crab Nebula where there is no evidence of dense matter [14] (other than the neutron star). Hence, we may be justified in neglecting the contribution of such nuclei to the γ-ray and neutrino production by hadronic collisions in comparison with the contribution from interactions of protons from neutron decay. However, some fraction of the energy of these nuclei could be transferred to very high energy electrons by resonant scattering [22]. Such electrons might then produce additional γ-rays by the SSC process as in the models discussed in ref. [2]. Hence, we suggest that the complex Crab Nebula spectrum may in fact be formed as a result of both processes, i.e. SSC and as a result of pulsar acceleration of nuclei discussed here.

Another consequence of our model is that particles (nuclei and protons from neutron decay) will be also injected by the Crab Pulsar and other pulsars into the Galactic cosmic rays, this may effect the cosmic ray spectrum and composition. This problem needs closer investigation, and should take into account the parameters of the Galactic population of pulsars at birth. However, it is worth noting that the energy distribution of the protons from decay of neutrons outside the Crab nebula peaks at $\sim 10^{15}$ eV (see Fig. 2), which is close to the energy of the knee in the cosmic ray spectrum.

[1] Nolan, P.L. et al. *Ap.J.* **409** 697 (1993); Much, R.P. et al. *A&A* **299** 435 (1995); de Jager, O.C. et al., *Ap.J.* **457** 253 (1996); Weekes, T.C. et al., *Ap.J.* **342** 379 (1989); Vacanti, G. et al., *Ap.J.* **337** 467 (1991).

[2] Gould, R.J., *Phys.Rev.Lett* **15** 577 (1965); Rieke, G.H., Weekes, T.C., *Ap.J.* **155** 429 (1969); Grindlay, J.E., Hoffman, J.A., *Astrophys. Lett.* **8** 209 (1971); Kundt, W., Krotschek, E., *A&A* **83** 1 (1980); de Jager, O.C., Harding, A.K., *Ap.J.* **396** 161 (1992); Aharonian, F., Atoyan, A., *Astropart. Phys.* **3** 275 (1995).

[3] Kwok, W.M., Cheng, K.S., Lau, M.M., *Ap.J.* **379** 653 (1991); Cheung, W.M., Cheng, K.S., *Ap.J.* **413** 694 (1993).

[4] Cheng, K.S., Cheung, T., Lau, M.M., Yu, K.N., Kwok, W.M., *J.Phys. G* **16** 1115 (1990).

[5] Karakuła, S., Tkaczyk, W., *Astropart. Phys.* **1** 229 (1993).

[6] Ho, C., *Ap.J.* **342** 396 (1989).

[7] Cheng, K.S., Ho, C., Ruderman, M., *Ap.J.* **300** 500 (1986); **300** 522 (1986).

[8] Stecker, F.W., *Phys.Rev.Lett.* **21** 1016 (1968).

[9] Chodorowski, M.J., Zdziarski, A.A., Sikora, M., *Ap.J* **400** 181 (1992).

[10] Goldreich, P., Julian, W.H., *Ap.J.* **157** 869 (1969).

[11] Manchester, R.N., Taylor, J.H., *Pulsars* (Freeman, San Francisco, 1977).

[12] Shapiro, S.L., Teukolsky, S.L., *Black Holes, White Dwarfs and Neutron Stars* (Ney York: Wiley, 1983).

[13] Atoyan, A.M., and Aharonian, F.A., *Mon. Not. R. Astr. Soc.* **278** 525 (1996).

[14] Davidson, K., Fesen, R.A., *ARAA* **23** 119 (1985).

[15] Hillas, A.H., in *Proc. 17th ICRC* (Paris) **8** 193 (1981).

[16] Lewis, D.A. et al., *Proc. 23rd ICRC* (Dublin) **1** 279 (1993).

[17] THEMISTOCLE collaboration, *Proc. 24th ICRC* (Rome) **2** 315 (1995).

[18] Tanimori, T., et al., *Ap.J.Lett.* submitted (1997).

[19] Amenomori, M. et al., *Proc. 24th ICRC* (Rome) **2** 346 (1995).

[20] Lipari, P., *Astropart. Phys.* **1** 195 (1993).

[21] Hester, J.J. et al., *Ap.J.* **448** 240 (1995).

[22] Hoshino, M., Arons, J., Gallant, Y.A., Langdon, A.B., *Ap.J.* **390** (1992) 454; Gallant, Y.A., Arons, J., *Ap.J.* **435** (1994).

TABLE I. Model parameters and limits on $\xi\mu$.

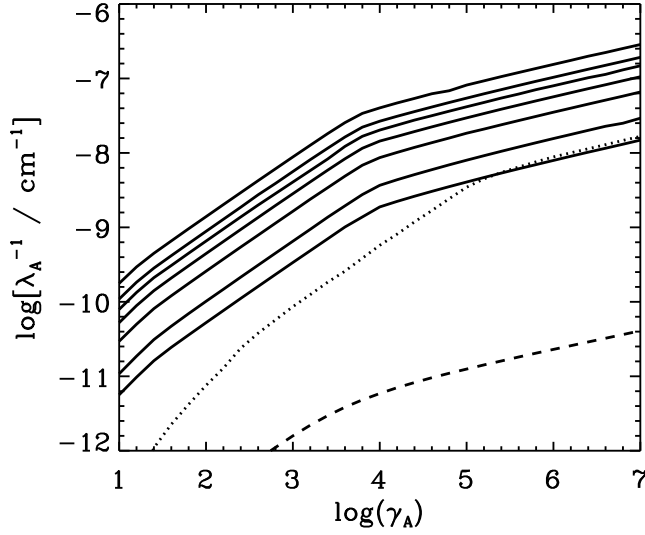| Model	I	II	III	IV
P_0 (ms)	5	10	10	10
r_{CN} (pc)	1	2	2	1
M_1	3	3	10	3
$(\xi\mu)_\gamma$ at 10 TeV	0.63	6.9	2.0	1.0
$(\xi\mu)_\nu$ at 10 TeV	0.22	1.8	0.54	0.29

FIG. 1. Reciprocal mean free paths for photodisintegration of nuclei with mass numbers, $A = 56, 40, 32, 24, 16, 8$, and 4 (full curves from the top) in the radiation field of the Crab pulsar's outer gap as a function of the Lorentz factor of the nuclei. The reciprocal mean free path for pion photoproduction (dotted curve) and the energy loss length for $e^{\pm}$ pair production (dashed curve) by iron nuclei are also shown.
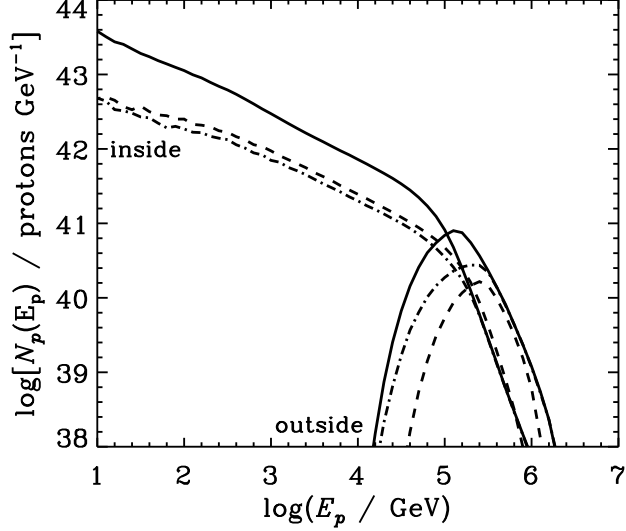
FIG. 2. Spectra of protons from the decay of neutrons injected by the Crab pulsar inside and outside the Crab Nebula assuming $M_1 = 3$ for the following parameters: $P_0 = 10$ ms, and Crab Nebula radius $r_{CN} = 1$ pc (dot-dashed curve) and 2 pc (dashed curve), and for $P_0 = 5$ ms and $r_{CN} = 1$ pc (full curve).
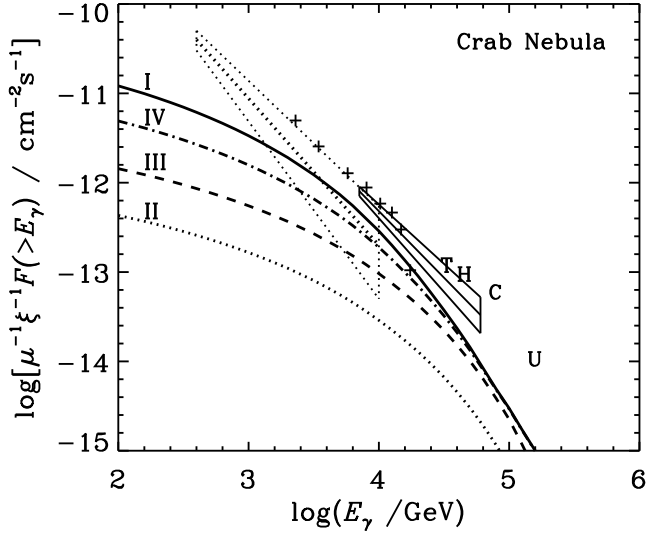
FIG. 3. Spectra of γ-rays from interactions of protons with matter inside the Crab Nebula for the different proton spectra shown in Fig 2 and for the different models of the nebula (I – IV) considered in the text. Observations: Whipple Observatory [16] (dotted line and error box); THEMISTOCLE [17] (+); and CANGAROO [18] (solid line and error box). Upper limits from various experiments mentioned in ref. [19]: T - Tibet, H - HEGRA, C - CYGNUS, and U - CASA-MIA.
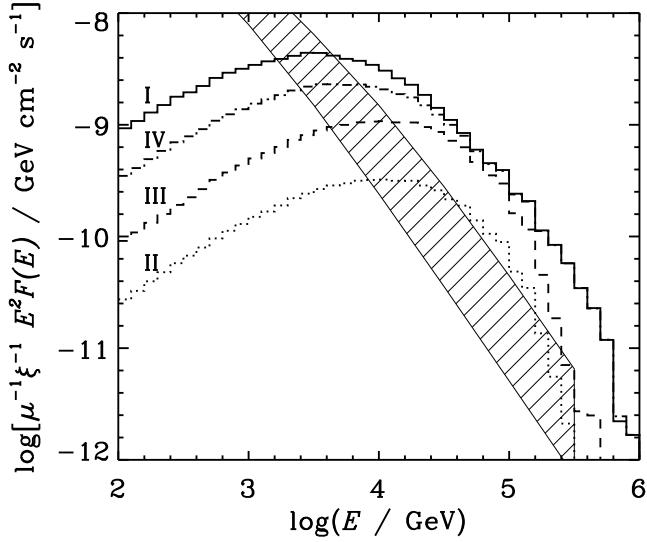

FIG. 4. Spectra of neutrinos ($\nu_\mu + \bar{\nu}_\mu$) expected for the different models (I - IV) considered in the text. The atmospheric neutrino background [20] within $1°$ of the source is indicated by the hatched band which shows the variation with angle: horizontal (upper bound), vertical (lower bound).